

# Digital Noise Reduction and Smoothing Technique: A Comparative Analysis of Gaussian smoothing, Isotropic Linear Diffusion, and Non-Linear Isotropic Diffusion smoothing

Sule Sani

Submitted: 20-06-2022

Revised: 29-06-2022

Accepted: 01-07-2022

## I. INTRODUCTION

A digital image is a representation of a real image that a digital computer may store and manipulate as a collection of numbers. The image is broken into tiny sections known as pixels so that it may be converted into numbers (picture elements). Today, an image is synonymous with a digital image and is crucial for everyday uses including computer tomography, satellite television, and medical imaging[1]. Different forms of sounds frequently adulterate the images captured by various types of devices and sensors. Hence To extract a reliable estimate of the original image from noisy states, image denoising is performed. mage denoising techniques are required to save crucial image elements like edges and texture while removing as much random additive noise as possible [2].

Different types of noise can contaminate digital photos. The data of interest may be compromised as a result of interference, issues with the data gathering procedure, and defective devices utilized in image processing. Additionally, transmission failures and compression can also generate noise[1]. Image denoising is the process of taking away noise from an image so that the original image can be seen. Denoised photos may necessarily lose some information since noise, edge, and texture are high-frequency components that are difficult to differentiate during the denoising process.

Several methods have recently tried to reconstruct noisy pixels using data from the overall image and have improved denoising performance. Block-matching 3D filtering (BM3D)[3],FFDNet [4], Deep Convolutional Neural Network [5], contourlet transform-based anisotropic diffusion filtering[6],Integer and Fractional-Order Total

Variation[7], Threshold, Wavelet Transform and Genetic Algorithm[8], principal component analysis with learned patch groups[9],Noise-Driven Anisotropic Diffusion Filtering[10] and their extensions are a few examples of typical algorithms used for denoising images. They are unable to effectively reduce salt and pepper noise, though. by incorporating Partial Differential Equations (PDE) we can denoise images for Image Restoration, Segmentation, Tracking, Estimation of the Optical Flow, and Registration.

In this study, we define and solve different Partial Differential Equations (PDE) while applying results using Gaussian smoothing, Isotropic linear diffusion smoothing, and Non-linear Isotropic diffusion. The result obtained from the comparative analysis is used to propose a good image denoising algorithm.

This paper is organized as follows:

- Introduction
- Literature review
- existing methods for image denoising
- Methods involved: the mathematical and implementation details
- Discussion of results
- Target audience - which research community is your work most relevant

## II. LITERATURE REVIEW

### A. Image Denoising problem

Image denoising can be mathematically expressed as:

$$x \square \square n \square \square \square \square \Psi \square \square$$

This represents a classic inverse problem. In equation (1), the unknown clean image is represented by  $x$ , the observed noisy image by  $\Psi$ , and the extra

noise by  $n$ . For modeling and assessing various denoising techniques  $n \sim N(0, \sigma^2)$ , or additional zero-mean Gaussian white noise, is typically used[11]. Now we can succinctly summarize the task of image denoising. We'd like to recover the clear image from a noisy image  $y$ . The reconstructed image is designated as  $x^c$ , with noise assumed to be  $n \sim N(0, \sigma^2)$ . Peak Signal to Noise Rate and Structure Similarity Index Measurement are two exemplary methods to assess a denoising method's effectiveness quantitatively. Visual quality comparisons across a group of photos are required even when quantitative measurements can't always accurately reflect the visual quality. For evaluating a denoising approach, edges and textures must be preserved in addition to the noise reduction effect[11].

### B. Existing Methods

There are two existing denoising methods namely: Local and non-local denoising methods. Local techniques use the pixels in a pixel's immediate vicinity to denoise it. Frequency domain and spatial domain techniques are examples of the traditional method[11].

#### i. Spatial domain Method

Denoising was initially done in the spatial domain using techniques including neighborhood filters, total variation, PDE-based algorithms, and

classic filters. These quick techniques tend to blur edges because they only use nearby neighbors to block out noise.

A typical isotropic filter is a gaussian filter. It calculates  $x^c$  as  $x^c = G_h * Y$ , where  $G_h$  is an established  $N \times N$  template. Averaging uses fixed weights that take into account no local structural variation. As a result, noise is removed by dramatically blurring edges. The Wiener filter is data-driven, in contrast to the Gaussian filter [12]. It produces an image  $x$  that is consistent with the minimization of the MSE (Mean Squared Error) between the estimated image and the original picture, i.e.,  $x^c = \min_x \text{MSE} = \min_x E (x^c - x)^2$ . The Wiener filter is adaptive since it is data-driven. The generalized Kalman filter for unstable signals is the Wiener filter[13].

An anisotropic diffusion model was proposed by Perona and Malik [14] This method is based on a partial differential equation (PDE). As can be seen, it adapts the diffusion speed in a pixel by the gradient's strength. Diffusion is thought to be isotropic in flat zones, however, it is primarily done along with tangent directions in edges or textural zones. Edges and textures can be kept while eliminating noise in flat zones. Another often used denoising technique is the curvature motion model. The key benefit of curvature motion is that it preserves edge information for contrast-invariant images[15].



Figure 1 Anisotropic diffusion model was proposed by Perona and Malik

Rudin and Osher's proposal for total variation integrates functional and attribute denoising with regularization into a general optimization framework[16]. Although it offers a crucial framework for picture denoising, it is too rigid for

realistic images and frequently produces too smoothed output. Then, many researchers suggest modified forms of total variation[17].

ii. Transform domain Method

The performance characteristics of imagesignal information and noise are different in the transform domain, which is an observation used by transform domain algorithms.

Some algorithms for picture denoising are presented and are based on the wavelet transform, a potent tool for image processing. Four categories can be used to group these techniques. It is first suggested how to extend the Wiener filter into the wavelet domain.[18], [19]. When applying the wavelet transform on a given noisy image, coefficients below a certain threshold are viewed as useful, while

coefficients above the threshold are viewed as noisy. There are two methods for dealing with these coefficients: hard thresholding and soft thresholding. Some approaches, such as SURE-based, Bayes-based, cross validation-based approaches, and others [20], [21], calculate an adaptive threshold rather than adopt an experimentally pre-selected threshold. Third, wavelet coefficients, including deterministic and statistical models, are thought to suit a certain distribution model. For the following purposes, non-orthogonal wavelet transforms are used for denoising.

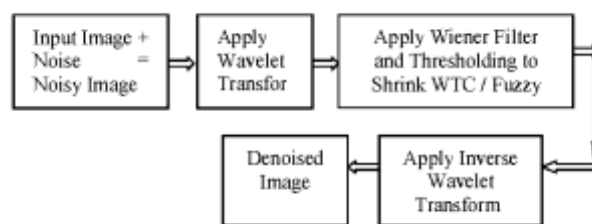


**Figure 2**Image de-noising using fuzzy and wiener filter in the wavelet domain

Data Adaptive Transformation methods such as ICA and PCA were used on provided noisy images. ICA (Independent Component Analysis) and PCA (Principal Component Analysis) are used as transform techniques[22]. The assumptions regarding the difference between signal and noise still hold since they are data adaptive.

iii. Sparse Representation Method

The origins of sparse representation can be found in compressive sensing[23], [24]. A patch can be sparsely represented, according to the theory of sparse representation, by a linear combination of

atoms in a redundant dictionary. Based on the sparse representation, Elad et al. presentedK-singular value decomposition (K-SVD)[25]. A natural picture dataset, the noisy image itself, or a predetermined transform like the discrete cosine transform (DCT) or wavelet transform can be used to train the vocabulary. Because it doesn't impose any smooth assumptions on the resulting image, the sparse representation-based method performs substantially better than earlier local methods. However, the borders are still fuzzy. Additionally suggested for maintaining details is improved K-SVD.

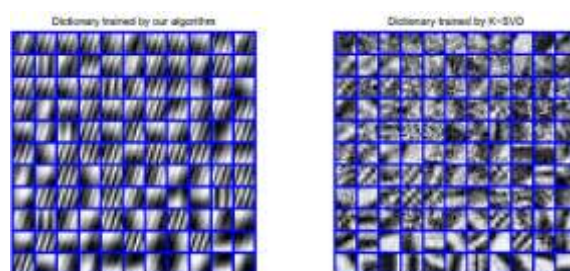


**Figure 3** Dictionary algorithm (left) and K-SVD algorithm (right)

Dictionary and sparse codes are typically updated iteratively. The first model has NP-hardness. The K-SVD and Method of Optimal Direction (MOD) dictionary updating algorithms are frequently used to effectively solve it [26]. The greedy algorithm and l1 norm convex relaxation are two efficient techniques for solving sparse codes. There are several greedy

algorithms, such as Matching pursuit, Orthogonal Matching Pursuit, Thresholding method, and Basis Pursuit andIteratively Reweighted Least Squares can solve the L<sub>1</sub> problem.

iv. Non-Local Scheme induced methods

Block Matching 3-D (BM3D) is a transform domain two-stage non-locally collaborative filter [27]. In each stage, it initially creates 3-D groups after collecting related patches by block matching for each patch in the image. Second, a wavelet or other transform is applied to each group to create the transform domain. Thirdly, a Wiener filter or hard-thresholding is applied to the coefficients. After all

recovered patches have been aggregated and the new coefficients have been translated back into the picture region, the entire image is estimated. A better version of BM3D is BM3D-SAPCA[28]. Particularly at low noise levels, they work extremely well. The visual quality of the recovered photos, however, is not great due to high noise levels. Particularly in flat locations, artifacts are introduced.

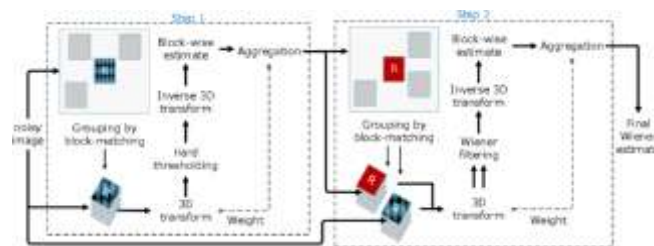


Figure 4 Adaptive Edge-guided Block-matching and 3D filtering (BM3D) Image Denoising Algorithm

Nonlocal self-similarity and sparse coding are combined into a single framework by LSSC (Learned Simultaneous Sparse Coding) [29]. On the codes of the collection of related patches, a grouped-Sparsity regularizes is imposed. Another effective technique that makes use of the nonlocal scheme and sparse representation is NCSR (Non-locally Centralized Sparse Representation)[30]. In contrast to LSSC, NCSR does not mandate that non-zero codes be placed in the same order inside a group. It encourages each patch to focus on the weighted average of the codes of other patches that are comparable to it. Even with high noise levels, it performs well, however, texture-redundant images will suffer from too much detail loss. The development of new denoising techniques is focused on edge restoration and texture preservation.

v. Deep Learning Method

The groundbreaking field of deep learning in image denoising is receiving a lot of attention. Several deep learning approaches are employed for the denoising process, however, those that deal with picture denoising differ in their subsequent steps.

Tian, et al. [31] give a succinct introduction of deep learning approaches (2020). In their research, more than 200 papers are evaluated for their contributions to the field of picture de-noising. The following is a summary of their major contributions:

- A demonstration of how deep learning techniques in practice affect image de-noising
- A summary of the deep learning techniques' responses to various noises
- Quantitative and qualitative evaluations of the effectiveness of deep learning's noise removal techniques.

- Specifying possible issues and future possibilities for deep learning in the area of image denoising

Most machine learning algorithms and deep learning techniques are built on top of neural networks. Neurons, input X, activation function f, weights, and biases b make up the majority of neural networks. A deep neural network is one with more layers than three. To get the desired results, artificial neural networks must be implemented carefully and with a lot of manual parameters. Deep convolutional neural networks (CNNs) were proposed as a result[32].

Due to their deep design and adaptable learning capabilities, convolutional neural networks have lately been adopted as the preferred method for picture denoising. Direct removal of SPN from the images is possible using Deep CNN[33]. They directly eliminate noise from images using CNNs, or convolutional neural networks. To eliminate salt and pepper noise from images, they used a multilayer CNN framework with padding, batch normalization, and rectified linear units. Three sets of photos were created: a training set, a validation set, and a test set. They discovered in their research that the model was capable of eradicating salt and pepper noise from a variety of photos.

It was also discovered that their architecture could only function well on photos having a lot of interference pixels. As a result, their use was broadened for the elimination of salt and pepper noise and led to effective outcomes. Deep CNNs have undoubtedly received a lot of attention, but they are not without drawbacks: (1) It is highly challenging to train a deep CNN for denoising, and (2) the majority of deep CNNs experience performance saturation[34]

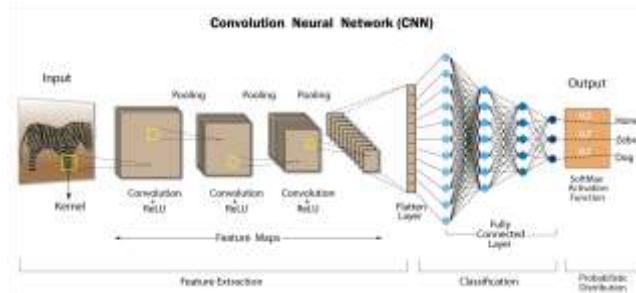


Figure 5 Convolutional Neural Network

Image denoising research is still in great demand due to its complexity and higher requirements. In terms of performance enhancement and speed acceleration, we suggest numerous research axes. The majority of sparsity-based models can effectively eliminate noise, but they struggle to maintain edges. On the one hand, it is important to continue researching the characteristics of edges and textures in noisy photos to maintain them well. For instance, denoising can be performed using models of natural image edges. On the other hand, non-local similarity measurement difficulty needs to be lowered to make non-local approaches more usable.

### III. METHODOLOGY

To better understand algorithms at their core, several algorithms are compared in this study. It also analyzes research employing various algorithms, including Gaussian smoothing, Isotropic linear

diffusion smoothing, and nonlinear isotropic diffusion smoothing. In this section, we discuss the methods in detail

#### A. Gaussian Smoothing

A 2-D convolution operator called the Gaussian smoothing operator is used to 'blur' images and eliminate noise and detail. It is comparable to the mean filter in this regard, but it makes use of a different kernel that simulates a Gaussian (or "bell-shaped") hump. The specific characteristics of this kernel are described below.

$$G(x) = \frac{1}{\sqrt{2\pi}\sigma} e^{-\frac{x^2}{2\sigma^2}} \quad (2)$$

where  $\sigma$  is the distribution's standard deviation. Additionally, we presupposed that the distribution's mean would be zero, centering it on the line  $x=0$ . Figure 6 shows the distribution in detail.

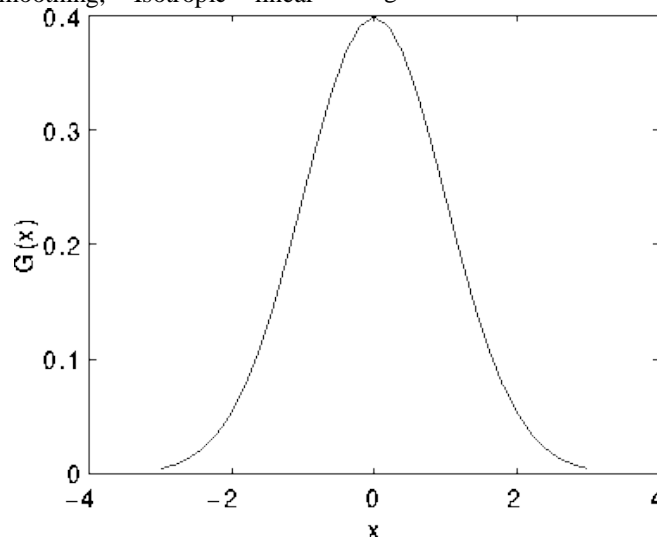
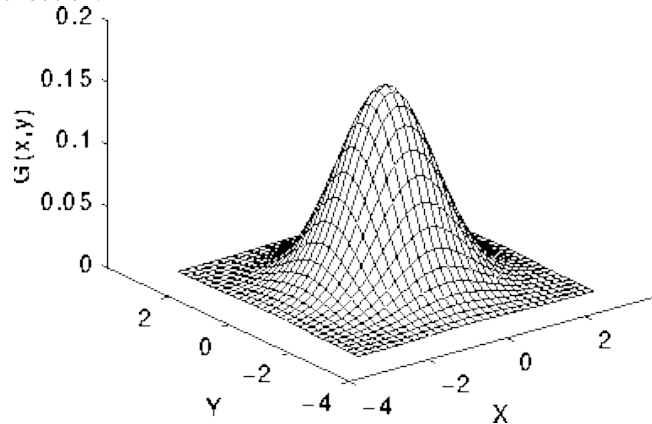


Figure 61-D Gaussian distribution with a mean of 0 and a  $\sigma$  value of 1

A circularly symmetric Gaussian in two dimensions (2D) has the shape:

$$G(x,y) = \frac{1}{\sqrt{2\pi}\sigma} e^{-\frac{x^2+y^2}{2\sigma^2}} \quad (3)$$

Figure 7 displays this distribution.



**Figure 7** Mean (0, 0) and  $\sigma=1$  in a two-dimensional Gaussian distribution

Convolution is used to accomplish the goal of Gaussian smoothing, which is to employ this 2-D distribution as a "point-spread" function. Before we can conduct the convolution, we must create a discrete approximation of the Gaussian function because the image is stored as a collection of discrete pixels. The Gaussian distribution is practically zero beyond around three standard deviations from the mean in practice, which allows us to truncate the convolution kernel at this point. In theory, the Gaussian distribution is non-zero everywhere, necessitating an arbitrarily large convolution kernel. An appropriate integer-valued convolution kernel that

closely resembles a Gaussian with an  $\sigma$  of 1.0 is shown in Figure 8. It is not immediately clear how to choose the mask's values to come close to a Gaussian.

One might use the Gaussian value at a pixel's center in the mask, but this is inaccurate because the Gaussian value varies nonlinearly throughout the pixel. Over the entire pixel, we integrated the Gaussian value (by summing the Gaussian at 0.001 increments). The array was rescaled so that the corners have the value 1, but the integrals are not integers. The 273 represents the total of all the values in the mask.

	1	4	7	4	1
	4	16	26	16	4
$\frac{1}{273}$	7	26	41	26	7
	4	16	26	16	4
	1	4	7	4	1

**Figure 8** Gaussian function discrete approximation with  $\sigma=1.0$

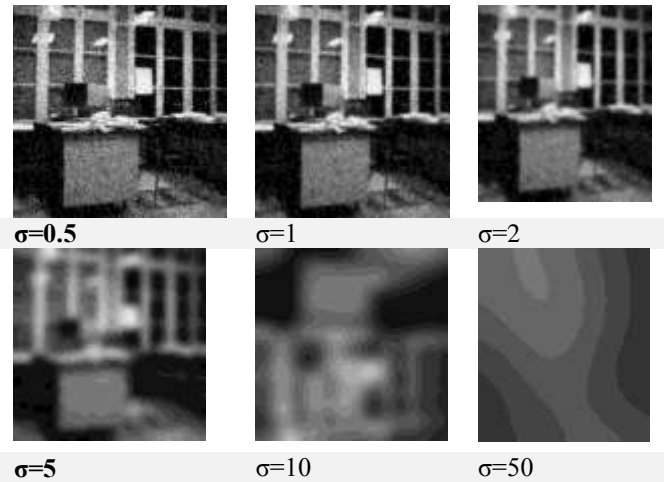
Once a suitable kernel has been determined, typical convolution techniques can be used to achieve the Gaussian smoothing. Since the equation for the 2-D isotropic Gaussian presented above can be divided into its x and y components, the convolution can be completed pretty quickly. To execute the 2-D convolution, one 1-D Gaussian in the x-direction must first be convolved, followed by another 1-D

Gaussian in the y-direction. Convoluting an image with a smaller Gaussian value numerous times is another method for computing a Gaussian smoothing with a high standard deviation. Even though this requires complicated computing, it may still be useful if a hardware pipeline is used for processing.

Hence, we Perform Gaussian smoothing on the input noisy "office" image by setting the kernel size

parameter to {0.5; 1; 2; 5; 10; 50}. The result of this computation is shown below:

**Table 1 Gaussian Smoothing result using different kernel parameter size**



The Gaussian distribution's variance, which establishes the amount of the blurring effect surrounding a pixel, is controlled by the value of  $\sigma$ . We experimented with sigma values ranging from 0.5 to 50 and found that as sigma increases, the amount of high-frequency information surrounding a pixel decreases. A larger kernel will blur the image more than a smaller kernel since a larger kernel has more values averaged into it.

Gaussian blurring has the secondary effect of denoising. The generated image may be helpful with little information loss if you choose tiny kernel sizes. However, information loss due to blurring may occur for large kernel sizes. Consequently, if edge preservation or texture information is important, Gaussian is typically not recommended for denoising.

As seen in  $\sigma = 50$ , increasing the standard deviation considerably attenuates high-frequency features (such as edges) while continuing to diminish or blur the intensity of the noise. Compared to a mean filter of comparable size, a gaussian filter offers softer smoothing and better maintains edges.

Denoising by Gaussian kernel is also called Gaussian smoothing because it is the result of blurring an image by a Gaussian function.

#### B. Isotropic Linear Diffusion Smoothing

The equation below describes the linear isotropic diffusion process:

$$\frac{\partial u}{\partial t} = \text{div}(d \nabla u)$$

$$u(x, y, 0) = I(x, y) \quad (4)$$

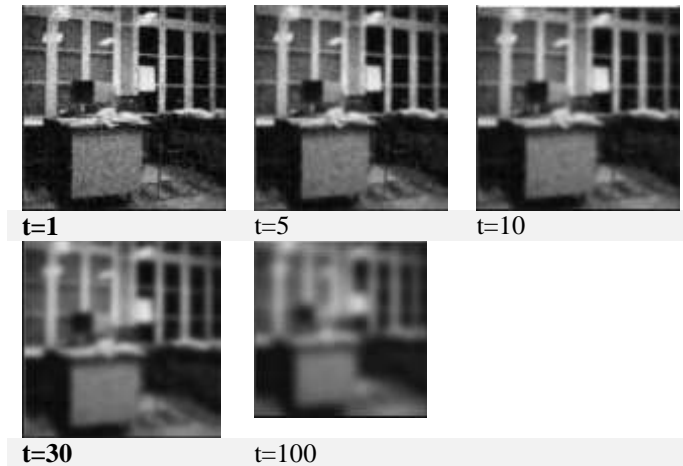
where  $I(x,y)$  is the initial noisy picture,  $u(x,y,t)$  is the image recovered after a diffusion period  $t$ , and  $d$  is a scalar constant diffusivity. Keep in mind that the evolving intensity distribution  $u(x,y,t)$  here corresponds to the evolving concentration distribution  $c(x,y,t)$ .

Isotropic diffusion is also known as a method for lowering picture noise without significantly altering the image's content. These elements often include edges, lines, and other characteristics crucial to the interpretation of the image. An image develops a parameterized family of gradually more and more blurred images based on a diffusion process in anisotropic diffusion, which is similar to the process that forms a scale space. Every image produced by this family is the result of convolution in the image with a 2D isotropic Gaussian filter, whose width rises as the parameter value does. The initial image is transformed linearly and spatially invariantly by the diffusion process.

This diffusion process is generalized by isotropic diffusion, which creates a family of parameterized images, each of which combines the original image with a filter that is dependent on the local content of the original image. Anisotropic diffusion is hence a non-linear and spatially variable change of the initial image. Hence, we Perform Isotropic Linear diffusion smoothing on the input noisy "office" image by setting the diffusion time

parameter to {1; 5; 10; 30; 100}. The result of this computation is shown below

**Table 2** Isotropic linear diffusion smoothing with diffusion time  $t$  at a different point



From table 2 it can be observed that the input image becomes less noisy and smoother as the diffusion time increases. The effect of increasing diffusion time  $t$  on the input image is observed as  $t$  increases it was found that the amount of high-frequency information surrounding a pixel decreases. Dirichlet boundary conditions should be used in this situation. The Dirichlet boundary condition is a sort of boundary condition used in the study of differential equations in mathematics. When applied to an ordinary or partial differential equation, it specifies the values that a solution must have throughout the domain's perimeter.

For a partial differential equation, for instance,  
 $\nabla^2 y + y = 0$  (6)

where  $\nabla^2$  denotes the Laplace operator, the Dirichlet boundary conditions on a domain  $\Omega \subset \mathbf{R}^n$  take the form

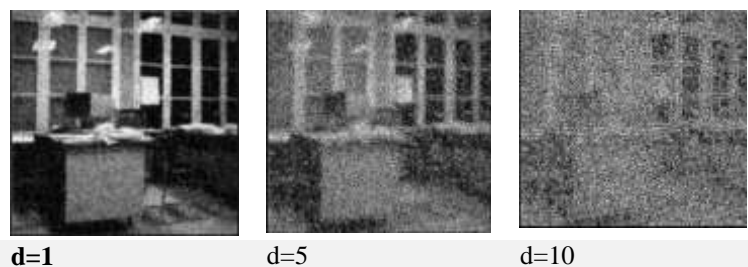
$$y(x) = f(x) \quad \forall x \in \partial\Omega. \quad (7)$$

where  $f$  is a known function defined on the boundary  $\partial\Omega$ .

The diffusion coefficient establishes how long a solute takes to diffuse across a specific distance in a medium.  $D$  has the area/time units, which are commonly  $\text{cm}^2/\text{s}$ . Each solute's value is different; hence it must be calculated empirically.

As the diffusion time increases the images get blurry and lose their edge. That is edge is not preserved as the diffusion time increases. Solving the diffusion PDE in equation (4) using  $d = \{1; 5; 10\}$  and comparing the output images at  $t = 10$ . We arrive at the solution result below:

At  $t = 1$



At  $t = 10$





Both at  $t=1$  and  $t=10$ , the input image at  $d = 1$  was denoised however as the value of  $d$  increased, it can be observed that the input image became very noisy and less smoother. It can be proved that a unique solution exists for the PDE in equation (4) which is given by:

$$u(x, y, t) = \begin{cases} I(x, y) & (t = 0) \\ (G_{\sqrt{2t}} * I)(x, y) & (t > 0) \end{cases} \quad (5)$$

where  $G_{2\pi}(x,y)$  is the Gaussian kernel. This proves that performing isotropic linear diffusion for a time  $t$  with  $d = 1$  is exactly equivalent to performing Gaussian smoothing with a  $\sigma = \text{SQRT}(2t)$ . We verify this fact using the noisy “office” image. For instance, when  $t=50$  and  $d=1$  it means  $\sigma = 10$ .

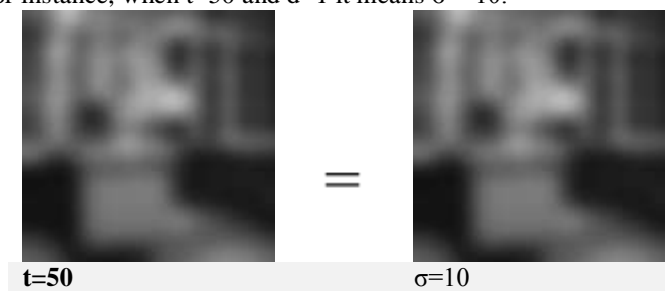


Figure 9 Proof of equation (5)

From figure 9 it can be concluded that performing isotropic linear diffusion for a time  $t$  with  $d = 1$  is exactly equivalent to performing Gaussian smoothing with a  $\sigma = \text{SQRT}(2t)$ .

### C. Non-Linear Isotropic Diffusion Smoothing

Partial Differential equations are the foundation of an entire area in image processing and computer vision (PDEs). Smoothing and picture restoration may be the key applications of PDE-based techniques in this field. Convoluting an image with a Gaussian kernel is a common technique for controlling linear diffusion to smooth an image.

Isotropic Non-Linear Diffusion strengthens outlines in photos and reduces noise. As object boundaries are reached, the diffusion coefficient locally adapts and disappears. The enhancement of object outlines and effective noise reduction

- Perona and Malik created the original version of NLDF (1987). It has several benefits:
- While little to no smoothing happens across image objects, noise is locally reduced in regions defined by object borders.

- Local edges are improved because borders and other discontinuities are magnified.

From a mathematical perspective, one can approach the issue as a diffusion process, where the diffusion coefficient is localized so that it ceases as soon as an object boundary is reached.

If we continue to use isotropic diffusion, we can only control the rate of diffusion; the direction of the diffusion is unaffected (thus we could truly think about this in 1D). Where the image is changing quickly, which is close to edge-like objects, less diffusion makes sense. This is possible with:

$$\frac{\partial u}{\partial t} = \text{div}(g(x)\nabla u) \quad (8)$$

To show that  $D$  is a scalar function of picture location, we have written it here as  $g(x)$ . In other words,  $g(x)$  is a diffusion that varies spatially. We obtain a linear PDE if  $g(x)$  only depends on the original image because in that case, it is effectively constant. A function that gets smaller with  $\nabla f_k$  would be a logical choice. Useful examples include:

$$g(\|\nabla f\|^2) = \frac{1}{\sqrt{1 + \frac{\|\nabla f\|^2}{\lambda^2}}} \quad (9)$$

Where constant  $\lambda > 0$ . Hence these decrease from 1 to 0 as the value for  $k\nabla f$  grows. When  $k\nabla f = \lambda$ , and

$$g = \frac{1}{2}. \quad (10)$$

As was already established, this results in artifacts because a little structure continues to affect the image even after it has vanished. It also seems unpleasant that, even after some smoothing, one point with the same  $k\nabla f$  will always undergo the same degree of smoothing while the other still has a high derivative. A ramp edge with extra noise wiggles could cause this.

Therefore, rather than relying on the initial image, we make  $g$  depend on the current, partially smoothed image.

$$g(\|\nabla u\|^2) = \frac{1}{\sqrt{1 + \frac{\|\nabla u\|^2}{\lambda^2}}} \quad (11)$$

This means that as we smooth, the degree of smoothing at each place is modulated by the gradient's current magnitude.

For denoising in this research, we take into account a non-linear isotropic diffusion process on an image domain. Following is a description of the non-linear isotropic diffusion process:

$$\frac{\partial u}{\partial t} = \text{div}(D \nabla u) \quad (12)$$

$$u(x, y, 0) = I(x, y)$$

Hence, we resolve equation (12) diffusion PDE. The noisy "office" image represents the starting situation. We, therefore, compute the results of the diffusion time  $t$  when  $t = \{5; 10; 30; 100\}$  in the form of photographs. Using  $\lambda = 0.5$ .

**Table 3 Nonlinear Isotropic diffusion smoothing with diffusion time  $t$  at a different point**

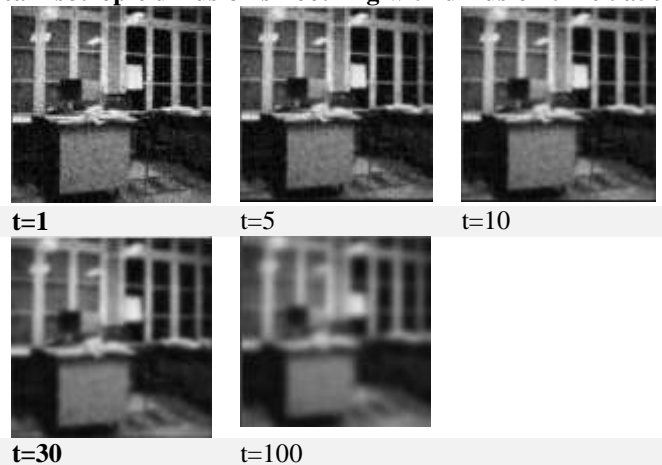
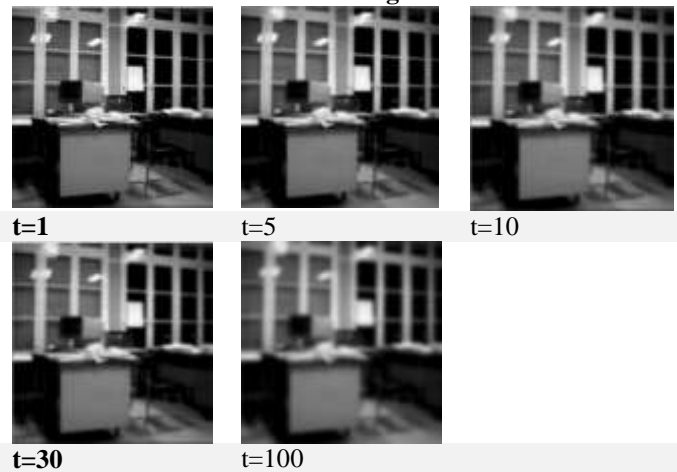


Table 3 result indicates a noise reduction in the processed input image. As the diffusion time increases the noise reduces while the contours in the image are enhanced. While there is little to no smoothing between image objects, noise is locally smoothed "inside" regions defined by object borders. Since borders and other discontinuities are amplified, local edges are strengthened.

Edge-preserving diffusion is non-linear diffusion with a diffusivity similar to the Perona-Malik diffusivity. This is because the Perona-Malik diffusivity is low when there are edges present, or when  $\nabla u$  is large  $D(x,y)$  is low. In this work, we Calculate the diffusivity  $D(x; y)$  on the office image that has no noise for the case where  $\lambda = 0.5$ , and display the diffusivity as a grayscale image. The outcome of this experiment is shown in table 4.

**Table 4 Nonlinear Isotropic diffusion smoothing with diffusion time  $t$  at a different point on a noiseless office image**



From the above images, it can be deduced that smoothing worked on the input image. The image output was smoothed and there is a strong indication of a strengthened edge. The edge strength of the present location, which depends on the differential structure of the image, is well captured by the gradient's length. This dependence makes the diffusion process nonlinear.

The edges obtained from non-linear isotropic diffusion smoothing in Tables 3 and 4 are well preserved compared to the edges in Isotropic Linear diffusion smoothing. This is because local edges are enhanced since discontinuities, such as boundaries, are amplified in non-linear isotropic diffusion smoothing. Using  $\lambda = \{0.5; 1; 2; 5; 10\}$  to solve the diffusion PDE in equation (12) and comparing the output images at  $t = 10$ . We have in table 5 and 6.

**Table 5 Non-Linear Isotropic Diffusion Smoothing at  $t=1$**

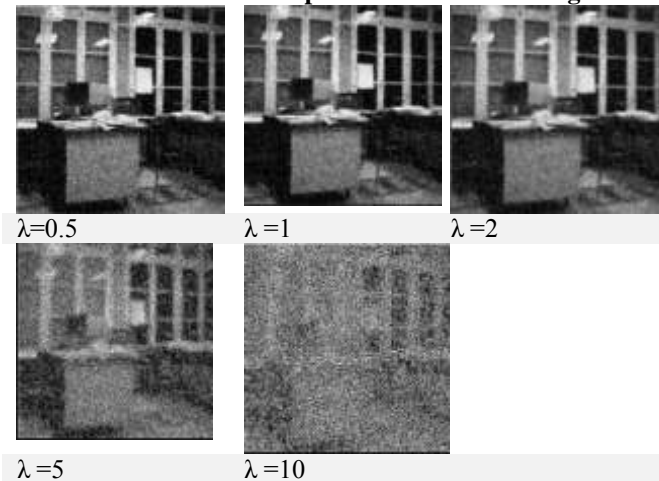
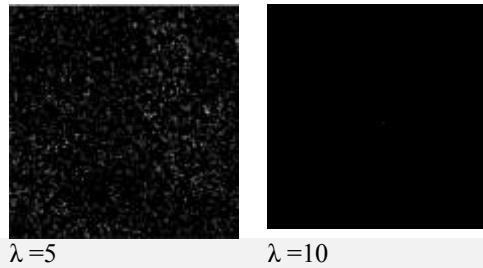


**Table 6 Non-Linear Isotropic Diffusion Smoothing at  $t=10$**





Compared to table 6, the output image in table 5 has preserved edges.  $\lambda$  reduced noise and smoothed the output image in table 5 than in table 6. Table 5 images and  $\lambda = 5$  and 10 increased the noise in the images. The increment in  $\lambda$  value in table 6 distorted the out image when  $\lambda = 2,5$  and 10. Hence  $\lambda$  has no significant effect on noise reduction at  $t = 10$ .

### DISCUSSION OF RESULTS

In this study, we discussed a few existing algorithms from two different categories of picture denoising techniques (local and nonlocal ones). Local approaches, as previously discussed, are quick but frequently result in blurring, particularly for edges and texture. Although slow, non-local approaches can produce results that are appealing to the eye. Recently, two effective and promising strategies are sparse representation and low rank. However, for this paper, our focus was on the comparison of Isotropic linear diffusion, Nonlinear Isotropic diffusion, and the Gaussian smoothing Algorithm.

Gaussian blurring has the secondary effect of denoising. The generated image may be helpful with little information loss if you choose tiny kernel sizes. However, information loss due to blurring may occur for large kernel sizes. Consequently, if edge preservation or texture information is important, Gaussian is typically not recommended for denoising.

Isotropic Non-Linear Diffusion strengthens outlines in photos and reduces noise. As object boundaries are reached, the diffusion coefficient locally adapts and disappears. The enhancement of object outlines and effective noise reduction. The research results prove nonlinear isotropic diffusion smoothing performs optimally in terms of edge preservation and Image denoising. From figure 9 it can be concluded that performing isotropic linear diffusion for a time  $t$  with  $d = 1$  is exactly equivalent to performing Gaussian smoothing with a  $\sigma = \text{SQRT}(2t)$ .

The edges obtained from non-linear isotropic diffusion smoothing in Tables 3 and 4 are well preserved compared to the edges in Isotropic Linear diffusion smoothing. This is because local edges are enhanced since discontinuities, such as boundaries, are amplified in non-linear isotropic diffusion smoothing.

### TARGET AUDIENCE

This research is relevant in the field of image processing. It solves problems like gap completion in biometric (Fingerprint) systems, medical imaging, digital forensics, computer-aided quality aided control, and other areas where image processing is required. The paper can be published on research gate, Springer, science direct, and even the IEEE (Institute of Electrical and Electronics Engineers) journal platform.

### REFERENCES

- [1] S. Roy, N. Sinha, and A. K. Sen, "a New Hybrid Image Denoising Method," *Int. J. Inf. Technol. Manag.*, vol. 2, no. 2, pp. 491–497, 2010, [Online]. Available: [http://www.csjournals.com/IJITKM/PDF\\_3-1/63.pdf](http://www.csjournals.com/IJITKM/PDF_3-1/63.pdf)
- [2] A. Fathi and A. R. Naghsh-Nilchi, "Efficient image denoising method based on a new adaptive wavelet packet thresholding function," *IEEE Trans. Image Process.*, vol. 21, no. 9, pp. 3981–3990, 2012, doi: 10.1109/TIP.2012.2200491.
- [3] M. Lebrun, "An Analysis and Implementation of the BM3D Image Denoising Method," *Image Process. Line*, vol. 2, pp. 175–213, 2012, doi: 10.5201/ipol.2012.1-bm3d.
- [4] A. Monod, J. Delon, and T. Veit, "An analysis and implementation of the hdr+ burst denoising method," *Image Process. Line*, vol. 11, pp. 142–170, 2021, doi: 10.5201/IPOL.2021.336.
- [5] F. Zhang, N. Cai, J. Wu, G. Cen, H. Wang, and X. Chen, "Image denoising method based on a deep convolution neural network," *IET Image Process.*, vol. 12, no. 4, pp. 485–493, 2018, doi: 10.1049/iet-ipr.2017.0389.
- [6] L. Jubairahmed, S. Satheeskumaran, and C. Venkatesan, "Contourlet transform based adaptive nonlinear diffusion filtering for speckle noise removal in ultrasound images," *Cluster Comput.*, vol. 22, pp. 11237–11246, 2019, doi: 10.1007/s10586-017-1370-x.
- [7] F. Kazemi Golbaghi, M. Rezghi, and M. R. Eslahchi, "A Hybrid Image Denoising Method

- Based on Integer and Fractional-Order Total Variation,” Iran. J. Sci. Technol. Trans. A Sci., vol. 44, no. 6, pp. 1803–1814, 2020, doi: 10.1007/s40995-020-00977-2.
- [8] Y. Liu, “Image Denoising Method based on Threshold, Wavelet Transform and Genetic Algorithm,” Int. J. Signal Process. Image Process. Pattern Recognit., vol. 8, no. 2, pp. 29–40, 2015, doi: 10.14257/ijcip.2015.8.2.04.
- [9] S. Routray, A. K. Ray, and C. Mishra, “An efficient image denoising method based on principal component analysis with learned patch groups,” Signal, Image Video Process., vol. 13, no. 7, pp. 1405–1412, 2019, doi: 10.1007/s11760-019-01489-2.
- [10] I. A. Artyukov and N. N. Irtuganov, “Noise-Driven Anisotropic Diffusion Filtering for X-Ray Low Contrast Imaging,” J. Russ. Laser Res., vol. 40, no. 2, pp. 150–154, 2019, doi: 10.1007/s10946-019-09782-8.
- [11] S. A. Solangi and Z. A. Dayo, “Image Denoising Methods : Literature Review Image Denoising Methods : Literature Review,” Int. J. Recent Res. Appl. Stud., vol. 32, no. July 2017, pp. 2–6, 2019.
- [12] N. Wiener, “Extrapolation, Interpolation, and Smoothing of Stationary Time Series,” Extrapolation, Interpolation, Smoothing Station. Time Ser., vol. 47, 2019, doi: 10.7551/mitpress/2946.001.0001.
- [13] R. E. Kalman, “A new approach to linear filtering and prediction problems,” J. Fluids Eng. Trans. ASME, vol. 82, no. 1, pp. 35–45, 1960, doi: 10.1115/1.3662552.
- [14] P. Perona and J. Malik, “Scale-Space and Edge Detection Using Anisotropic Diffusion,” IEEE Trans. Pattern Anal. Mach. Intell., vol. 12, no. 7, pp. 629–639, 1990, doi: 10.1109/34.56205.
- [15] B. Merriman and J. Bence, “Diffusion generated motion by mean curvature,” Math.Ucla.Edu, 1992, [Online]. Available: ftp://ftp.math.ucla.edu/pub/camreport/cam92-18.pdf%5Cnpapers3://publication/uuid/F87E4678-DCBA-492B-AAAD-1BD538C24DBB
- [16] L. I. Rudin, S. Osher, and E. Fatemi, “Nonlinear total variation based noise removal algorithms,” Phys. D Nonlinear Phenom., vol. 60, no. 1–4, pp. 259–268, 1992, doi: 10.1016/0167-2789(92)90242-F.
- [17] T. Chan, S. Esedoglu, F. Park, and A. Yip, “Total variation image restoration: Overview and recent developments,” Handb. Math. Model. Comput. Vis., pp. 17–31, 2006, doi: 10.1007/0-387-28831-7\_2.
- [18] V. Strela, “Denoising Via Block Wiener Filtering in Wavelet Domain,” Eur. Congr. Math., pp. 619–625, 2001, doi: 10.1007/978-3-0348-8266-8\_55.
- [19] H. Zhang, A. Nosratinia, and R. O. Wells, “Image denoising via wavelet-domain spatially adaptive FIR Wiener filtering,” ICASSP, IEEE Int. Conf. Acoust. Speech Signal Process. - Proc., vol. 4, pp. 2179–2182, 2000, doi: 10.1109/ICASSP.2000.859269.
- [20] M. Jansen, “Wavelets and wavelet thresholding,” New York, NY Springer New York, pp. 9–45, 2001, doi: 10.1007/978-1-4613-0145-5\_2.
- [21] E. P. Simoncelli and E. H. Adelson, “Noise removal via Bayesian wavelet coring,” IEEE Int. Conf. Image Process., vol. 1, pp. 379–382, 1996, doi: 10.1109/icip.1996.559512.
- [22] L. Zhang, W. Dong, D. Zhang, and G. Shi, “Two-stage image denoising by principal component analysis with local pixel grouping,” Pattern Recognit., vol. 43, no. 4, pp. 1531–1549, 2010, doi: 10.1016/j.patcog.2009.09.023.
- [23] E. J. Candès, “The restricted isometry property and its implications for compressed sensing,” Comptes Rendus Math., vol. 346, no. 9–10, pp. 589–592, 2008, doi: 10.1016/j.crma.2008.03.014.
- [24] D. L. Donoho, “Compressed sensing,” IEEE Trans. Inf. Theory, vol. 52, no. 4, pp. 1289–1306, 2006, doi: 10.1109/TIT.2006.871582.
- [25] M. Elad and M. Aharon, “Image denoising via sparse and redundant representations over learned dictionaries,” IEEE Trans. Image Process., vol. 15, no. 12, pp. 3736–3745, 2006, doi: 10.1109/TIP.2006.881969.
- [26] K. Engan, S. O. Aase, and J. H. Husoy, “Method of Optimal Directions for frame design,” ICASSP, IEEE Int. Conf. Acoust. Speech Signal Process. - Proc., vol. 5, pp. 2443–2446, 1999, doi: 10.1109/icassp.1999.760624.
- [27] K. Dabov, A. Foi, and K. Egiazarian, “Video denoising by sparse 3D transform-domain collaborative filtering,” Eur. Signal Process. Conf., pp. 145–149, 2007.
- [28] K. Dabov, R. Foi, V. Katkovnik, and K. Egiazarian, “BM3D image denoising with shape-adaptive principal component analysis,” Proc. Work. Signal Process. with Adapt. Sparse Struct. Represent., p. 6, 2009.
- [29] J. Mairal, F. Bach, J. Ponce, G. Sapiro, and A. Zisserman, “Non-local sparse models for image restoration,” Proc. IEEE Int. Conf. Comput. Vis., pp. 2272–2279, 2009, doi: 10.1109/ICCV.2009.5459452.
- [30] W. Dong, L. Zhang, G. Shi, and X. Li,

- “Nonlocally centralized sparse representation for image restoration,” *IEEE Trans. Image Process.*, vol. 22, no. 4, pp. 1620–1630, 2013, doi: 10.1109/TIP.2012.2235847.
- [31] C. Tian, L. Fei, W. Zheng, Y. Xu, W. Zuo, and C. W. Lin, “Deep learning on image denoising: An overview,” *Neural Networks*, vol. 131, pp. 251–275, 2020, doi: 10.1016/j.neunet.2020.07.025.
- [32] Y. Yao, X. Wu, L. Zhang, S. Shan, and W. Zuo, “Joint representation and truncated inference learning for correlation filter based tracking,” *Lect. Notes Comput. Sci. (including Subser. Lect. Notes Artif. Intell. Lect. Notes Bioinformatics)*, vol. 11213 LNCS, pp. 560–575, 2018, doi: 10.1007/978-3-030-01240-3\_34.
- [33] Y. Xing, J. Xu, J. Tan, D. Li, and W. Zha, “Deep CNN for removal of salt and pepper noise,” *IET Image Process.*, vol. 13, no. 9, pp. 1550–1560, 2019, doi: 10.1049/iet-ipr.2018.6004.
- [34] C. Tian, Y. Xu, and W. Zuo, “Image denoising using deep CNN with batch renormalization,” *Neural Networks*, vol. 121, pp. 461–473, 2020, doi: 10.1016/j.neunet.2019.08.022.